URSI AP-RASC, Sydney, Australia, 17 – 22 August 2025

Coherence estimation of UAS-SAR images by varying the synthetic aperture in controlled and natural scenarios

Alessandra Beni, Lapo Miccinesi, Luca Bigazzi, Lorenzo Pagnini, Andrea Cioncolini, Massimiliano Pieraccini*
Department of Information Engineering (DINFO), University of Florence, via Santa Marta 3, 50139 Firenze Italy

Abstract

Unmanned aerial system (UAS)-based Synthetic Aperture Radars (SAR) represent flexible and cost-effective solutions for environmental monitoring and are a promising technology in the field of remote sensing. One of the main applications is interferometry, which allows the detection of ground displacements with high precision. Unlike ground-based or satellite systems, flight instabilities of UAS-based SAR could severely affect image processing. Specifically, the interferometric performance strongly depends on the scan length used to process the SAR image, the so-called synthetic aperture. This paper presents an experimental study on UAS-based SAR performance in terms of image quality and temporal coherence, with a focus on the role of the synthetic aperture length.

1. Introduction

Unmanned aerial systems (UASs) are gaining lot of attention as synthetic aperture radar (SAR) platforms. In recent years lot of research have been focused on UAS-based SAR systems [1]. They offer short and versatile revisit times together with flexible acquisition geometries that are not achievable with space-borne, airborne, or ground-based SAR systems. Repeat-pass interferometry is a promising application of UAS-based SAR system, which allows to measure ground deformations with sub-millimeter precision. However, UAS-based SAR interferometry is particularly challenging due to flight stability issues. For example, in the presence of wind, UAS often deviates from the nominal straight trajectory. Recently, research has focused on the performance of UAS-based SAR systems analyzing the impact of flight speed on SAR images [2], [3], and its peculiar acquisition geometry [4]. Several experimental works presented interferometric measurements performed using S-band [5], L-band [6], [7], and Ku-band [8] UAS-based SAR systems.

Temporal coherence of SAR images is critical to perform repeat-pass interferometric measurements: high coherence is required to obtain reliable interferograms. The temporal decorrelation has been largely studied for space-borne [9], [10] and ground-based SAR [11], [12] especially in vegetated and forested areas, since it is fundamental to assess the interferometric performance.

This paper presents an experimental study on the quality and temporal coherence of S-band UAS-based SAR images. It has been shown that the interferometric accuracy strongly depends on the length of the sub-synthetic aperture (SSA) used for UAS-based SAR image processing [5]. The shorter the SSA, the smaller the displacement error. At the same time, a longer SSA corresponds to a higher cross-range resolution. The choice of the SSA length is therefore crucial and determines many of the characteristics of the resulting SAR image. In this work, we analyze the temporal decorrelation of S-band UAS-based SAR acquisitions, together with the image quality, while varying the SSA length. This study can provide important insights for optimal processing of UAS-based data. Two measurements campaigns were performed: in a controlled scenario, a general aviation airfield, and on a slope with natural vegetation in a former quarry area.

2. Methodology

The acquired radar data was focused using the back propagation algorithm (BPA) introduced in [5]. This SAR processing is based on the definition of a SSA length. For each pixel of the SAR image, the SSA outlines the portion of the total synthetic aperture to be processed, as illustrated in Figure 1. The choice of SSA length is limited by uncertainty on the estimated trajectory. Indeed, if the trajectory is not estimated exactly, increasing the SSA introduces more noise into the image.

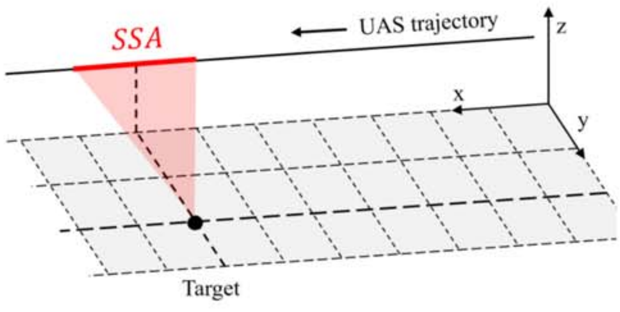

Figure 1. Definition of the SSA in the back propagation algorithm described in [5].

In this paper, SAR data was processed using different values of SSA to evaluate its impact on the quality of the image. To determine the imaging performance as the SSA length varies, two parameters have been evaluated: the peak-to-sidelobe ratio and the amplitude dispersion index. The peak-to-sidelobe ratio (PSLR) of a target signal is a measure of the peak amplitude value with respect to the sidelobes. It is defined as [13]

$$PSLR = 20\log_{10}\left(\frac{peak(A) - \mu(A_{sidelobe})}{\sigma(A_{sidelobe})}\right). \quad (1)$$

Here, $peak(A)$ is the peak amplitude value, while $\mu(A_{sidelobe})$ and $\sigma(A_{sidelobe})$ are, respectively, the mean and standard deviation of signal amplitude, evaluated in the sidelobe region. The sidelobe region was selected as the region beyond the minimum closest to the peak. A high $PSLR$ corresponds to a high signal compared to the surrounding environment, i.e. a high signal-to-noise ratio. The amplitude dispersion index has been shown to provide useful information on the temporal coherence of a radar image [12]. It is also easier to calculate than coherence estimators. The amplitude dispersion index is defined as

$$D_A = \frac{\sigma_A}{\mu_A}. \quad (2)$$

Here, A is the amplitude of the signal of a target, σ_A and μ_a the standard deviation and mean value, respectively, of the signal amplitude time series. In this article this parameter is evaluated for the CR signal in order to quantify the level of temporal decorrelation of the image time series.

3. System and test sites

The UAS-based SAR system used for this study is described in [5]. This radar is based on a Vector Network Analyzer (VNA) that provides a continuous-wave stepped-frequency (CWSF) signal with central frequency of 4.05 GHz and a pulse repetition frequency of 60 Hz. The radar can provide a bandwidth of 60-100 MHz, with a number of frequency samples equal to 201. The SAR linear scan is performed as follows: the UAS flies sideways to the interested area at a velocity of 1 m/s, with the radar antennas pointed orthogonal to the flight direction.

Two kinds of scenarios were investigated: a general aviation airfield and a natural slope in a former quarry area. In both cases, a CR with sides of 50 cm was placed at the center of the scenario. The general aviation airfield is located near Castiglion Fiorentino, Arezzo, Italy. In these measurements, the UAS flew at an altitude of 5 m on the ground following a linear trajectory. The total scan length was 100 m long. The radar bandwidth was set to 100.5 MHz. The resulting range resolution was approximately 1.5 m. A picture of the measurement site is shown in Figure 2. The CR was located on a meadow, on a tripod, far from other targets in the scenario.

The natural scenario was located near Firenzuola, Italy. Figure 3 shows the illuminated area: a slope with vegetation and rocks. A CR was placed on the slope. The UAS flew at an altitude of about 20 m above the starting point, approximately the same height as the CR. The scan was about 60 m long. The radar bandwidth was set to 67 Hz. This ensured an unambiguous range of about 450 m, which was essential for this scenario. The resulting range resolution was approximately 2.24 m. In this case, the CR was not isolated, but it was positioned near other natural targets: a tree and some rocks.

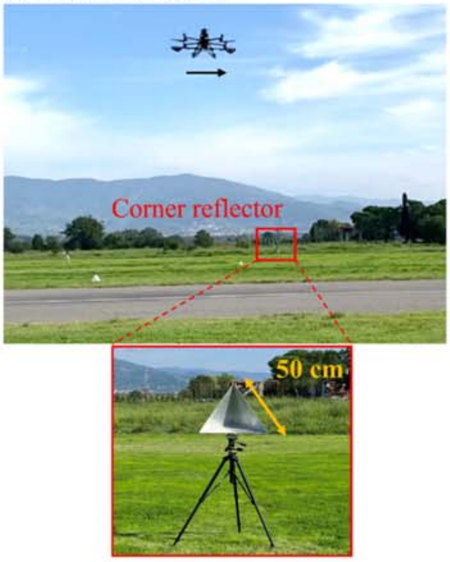

Figure 2. Test site in controlled scenario: UAs performening the scan and corner reflector.

Figure 3. Test site in the natural scenario.

4. Measurements results

SAR images have been processed with BPA described in [5] and [3], while varying the SSA. The $PSLR$ of the CR signal was evaluated using (1) for the two scenarios. Figure 4 shows the obtained results for several values of the SSA length, from 7 m to 60 m, the total length of the scan in the natural scenario. The two curves show a similar trend but different values. For SSA from 7 m to approximately 15-20 m, the $PSLR$ increases. Indeed, while increasing the SSA, more data contributes to the peak signal, and its value increases. After a critical value, a further increase of the SSA does not correspond to a $PSLR$ increase. For the controlled scenario, it saturates at an almost constant value (36 dB) for SA > 20 m. In the natural scenario, after SSA ≃ 20 m, the $PSLR$ slightly decreases again. In fact, further widening the SSA adds noise due to flight instability and motion errors caused by uncertainties in the retrieved trajectory. It can be observed that in the natural scenario the CR signal assumes lower values (from 21 dB to about 22-23 dB) compared to the CR signal acquired in controlled scenario (from 25 dB to 36 dB). Indeed, in the first case the CR was not isolated from other targets.

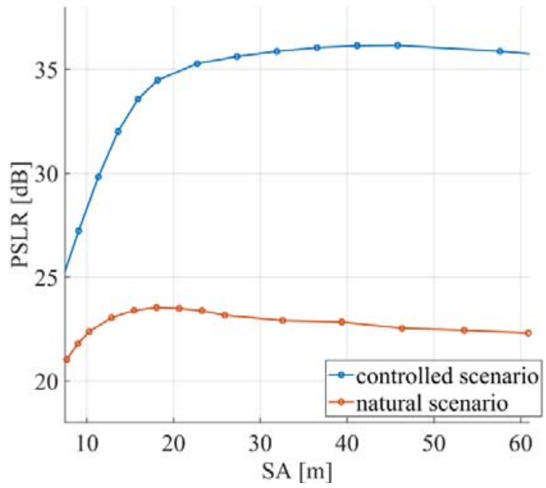

Figure 4. PSLR of the CR signal in the natural and controlled scenario, as a function of the SSA length.

For the two measurement campaigns, the D_A (2) of the CR signal was evaluated as a function of the SSA length used to focus the image. The results are shown in Figure 5. For the controlled scenario (blue line), the value of D_A increases with SSA. This means that widening the SSA adds a certain degree of noise to the image, due for instance to trajectory errors. The longer the SSA length, the more signal decorrelation in the resulting image. However, it should be noted that the value of D_A in controlled scenario is always less than 0.25, the limit value below which the signal can be considered coherent. The D_A of the CR in the natural scenario shows a different trend. The D_A value assumes the lowest value ($D_A = 0.18$), which corresponds to maximum coherence, for SSA = 7 m. Then, the parameter increases up to 0.38 for SSA $\simeq$ 18 m. After this value, the parameter decreases again and has a local minimum for SSA= 39.4 m ($D_A = 0.26$). This behavior is probably due to the contribution of two factors: signal decorrelation due to flight instabilities and trajectory errors, and better cross-range resolution for longer SSA. Theoretically, the relation between the SSA length and the cross-range resolution Δx of the radar image is given by

$$\Delta x = \frac{\lambda}{2\,SA} \qquad (3)$$

where λ is the wavelength associated to the central frequency of the radar signal. Indeed, the natural scenario is characterized by the presence of multiple scatterers near to the CR. With poor cross-range resolution, multiple targets belong to the same resolution cell, and their signals are summed up, which results in a decrease of signal coherence. As cross-range resolution increases, signals backscattered by different targets are separated in different resolution cells, and the signal coherence increases. Since in controlled scenario the CR was isolated from other targets, this effect is not evident and is dominated by decorrelation due to trajectory errors.

Given the above results, it can be deduced that a change in the range resolution should also have an impact on signal coherence. The range resolution of a radar image depends on the signal bandwidth B according to

$$\Delta y = \frac{c}{2\,B} \qquad (4)$$

with c the speed of light. The D_A of the CR signal was also calculated while varying the radar bandwidth, with fixed SSA = 32 m. Specifically, the bandwidth was decreased from the maximum value, by taking less frequency samples, down to 10 MHz. Figure 6 shows the results obtained in the two scenarios. It can be observed that in both cases D_A decreases (coherence increases) while B increases, i.e. while resolution improves. Improving the range resolution leads to an increase in signal coherence even in controlled scenario for isolated targets.

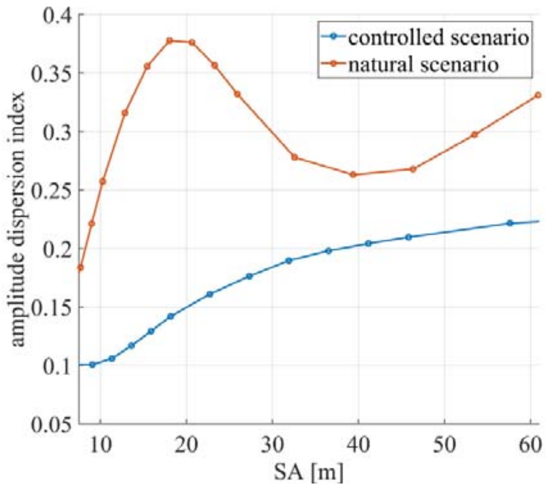

Figure 5. $\boldsymbol{D_A}$ as a function of the SSA length of the CR signal in the controlled (blue) and natural (red) scenario.

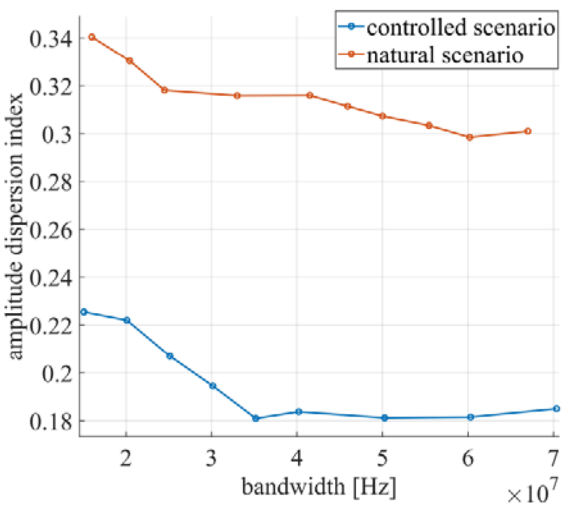

Figure 6. $\boldsymbol{D_A}$ of the CR signal as a function of B in the controlled (blue) and natural (red) scenario.

5. Conclusions

This paper presents a study on the performance of a UAS-based S-band SAR system. To perform interferometric measurements high quality and high coherence of SAR images is crucial. This paper experimentally investigates the relation between signal coherence and processed synthetic aperture length in two specific case studies. The peak-to-sidelobe ratio was used to determine the degree of image quality and was shown to improve as the synthetic aperture length increased, especially for isolated targets. By evaluating the dispersion index of the signal amplitude of a corner reflector, the coherence of the signal was estimated. It was observed that, in general, increasing the sub-synthetic aperture reduces signal coherence. However, the image resolution also impacts on image coherence: a higher resolution implies a lower decorrelation. Results showed that to achieve maximum coherence and obtain reliable interferograms, both sub-synthetic aperture and resolution must be taken into account.

6. Acknowledgement

This work has been partially supported by ASTRA (Autonomous unmanned aerial System for synThetic aperture Radar, photogrAmmetry and digital image correlation) project n° 20228YYR5Z, PRIN2022 (Progetti di Rilevante Interesse Nazionale), in the framework of the funding by the Italian Ministero dell'Università e della Ricerca, European Union NextGenerationEU.

References

[1] L. Miccinesi, A. Beni, and M. Pieraccini, 'UAS-Borne Radar for Remote Sensing: A Review', Electronics, vol. 11, no. 20, Art. no. 20, Jan. 2022, doi: 10.3390/electronics11203324.

[2] Y. Shigemitsu, K. Ishitsuka, W. Lin, T. Sugiyama, M. Kishimoto, and T. Takahashi, 'Effect of drone flight speed on intensity images in drone-based synthetic aperture radar analysis of mine slopes', Remote Sensing Letters, vol. 15, no. 6, pp. 591–602, Jun. 2024, doi: 10.1080/2150704X.2024.2354070.

[3] A. Beni, L. Miccinesi, and M. Pieraccini, 'UAS-borne CWSF SAR imaging: evaluation and compensation of Doppler effect', in 2023 IEEE International Radar Conference (RADAR), Nov. 2023, pp. 1–5. doi: 10.1109/RADAR54928.2023.10371049.

[4] W. Tian, X. Xie, Y. Deng, Z. Yang, and C. Hu, 'A Modified Interferometric Phase Model for Imaging Integral Angle Applied to UAV InSAR', IEEE Transactions on Geoscience and Remote Sensing, pp. 1–1, 2024, doi: 10.1109/TGRS.2024.3388421.

[5] A. Beni, L. Miccinesi, L. Pagnini, L. Bigazzi, A. Cioncolini, and M. Pieraccini, 'UAS-Based SAR Repeat-Pass Interferometry With Ground Truth', IEEE Access, vol. 12, pp. 48797–48806, 2024, doi: 10.1109/ACCESS.2024.3383539.

[6] S.-Y. Jeon et al., 'Experimental Demonstration of Bistatic UAV-Borne SAR and InSAR', in EUSAR 2024; 15th European Conference on Synthetic Aperture Radar, Apr. 2024, pp. 1150–1155. Accessed: Dec. 12, 2024. [Online]. Available: https://ieeexplore.ieee.org/abstract/document/10659473

[7] O. Frey and C. L. Werner, 'UAV-borne repeat-pass SAR interferometry and SAR tomography with a compact L-band SAR system', in EUSAR 2021; 13th European Conference on Synthetic Aperture Radar, Mar. 2021, pp. 1–4. Accessed: Jan. 15, 2024. [Online]. Available: https://ieeexplore.ieee.org/abstract/document/9472527

[8] G. Ruiz-Carregal et al., 'Ku-Band SAR-Drone System and Methodology for Repeat-Pass Interferometry', Remote Sensing, vol. 16, no. 21, Art. no. 21, Jan. 2024, doi: 10.3390/rs16214069.

[9] P. Tang, W. Zhou, B. Tian, F. Chen, Z. Li, and G. Li, 'Quantification of Temporal Decorrelation in X-, C-, and L-Band Interferometry for the Permafrost Region of the Qinghai–Tibet Plateau', IEEE Geoscience and Remote Sensing Letters, vol. 14, no. 12, pp. 2285–2289, Dec. 2017, doi: 10.1109/LGRS.2017.2761900.

[10] Y. Endo et al., 'Comparison of Temporal Decorrelation Decay Functions Over Land Cover Types for L- and C-Band SAR', in IGARSS 2024 - 2024 IEEE International Geoscience and Remote Sensing Symposium, Jul. 2024, pp. 10719–10722. doi: 10.1109/IGARSS53475.2024.10642568.

[11] A. Monti-Guarnieri, M. Manzoni, D. Giudici, A. Recchia, and S. Tebaldini, 'Vegetated Target Decorrelation in SAR and Interferometry: Models, Simulation, and Performance Evaluation', Remote Sensing, vol. 12, no. 16, Art. no. 16, Jan. 2020, doi: 10.3390/rs12162545.

[12] A. Beni, L. Miccinesi, A. Michelini, and M. Pieraccini, 'Temporal Coherence Estimators for GBSAR', Remote Sensing, vol. 14, no. 13, Art. no. 13, Jan. 2022, doi: 10.3390/rs14133039.

[13] M. Sawides, B. V. K. V. Kumar, and P. K. Khosla, '"Corefaces" - robust shift invariant PCA based correlation filter for illumination tolerant face recognition', in Proceedings of the 2004 IEEE Computer Society Conference on Computer Vision and Pattern Recognition, 2004. CVPR 2004., Jun. 2004, p. II–II. doi: 10.1109/CVPR.2004.1315251.